Felix Pressler

Lattice Spectroscopy of Strongly Interacting Dark Matter Candidates

Bachelor's Thesis

in partial fulfillment of the requirements for the degree of

Bachelor of Science - BSc

in Physics

submitted to

University of Graz
Graz University of Technology

Supervisor

Univ.-Prof. Dipl.-Phys. Dr.rer.nat. Axel Maas

Co-Supervisor

Fabian Zierler, BSc MSc

Institute of Physics

Graz, July 2022

Abstract

The search for dark matter aims at answering fundamental questions about the workings and the contents of our universe. While a common paradigm over the last few decades suggested that dark matter might only be weakly interactive, this work explores the possibility of strong self interactions in dark particles. For this, a recently proposed QCD-like gauge theory with gauge group $Sp(4)$ is introduced. Simulation data of the corresponding fields on a space-time lattice is analysed with respect to the correlation functions of the dark mesonic particles. A strategy for fitting said correlators is established and tested with already analysed data, in order to extract the particle masses. The correlators of a single meson as well a scattering state of two particles are then looked into, while extracting the ground state energies as well as the scattering length of the latter state. The resulting cross section is compared to astrophysically observed constraints and assessed accordingly. It is found that not only the correlation functions of the observed states are useful tools for this type of evaluation but the probed theory also provides a viable framwork for describing potential candidates for strongly interacting dark matter.

Contents

1 Introduction

Without a doubt it can be said that the search for dark matter comprises some of the most captivating riddles modern physics has yet to answer. Behind a veil of technical terms lies nothing less than the questions about how gravity works, what the universe is made of and which approaches can guide us in answering them.

This work aims at helping to probe the nature of dark matter as well as finding valuable tools to do so. For this, a recently described QCD-like gauge theory with gauge group $Sp(4)$ is introduced, providing a framework to describe dark particles that interact strongly. This setting is then transferred on a lattice, where simulations have been done regarding the behaviour of the dark quark fields.

The main part of this work then consists of analysing the correlation functions of the corresponding mesonic particles. From these quantities, the ground state energy of the individual states can be extracted, signifying the mass of the particle.

Furthermore, an extreme low energy s-wave scattering state of two dark pions with isospin 2 is analysed, from which the scattering length is estimated. The cross section is calculated, providing a helpful measure of the interaction between the assumed dark particles. This quantity is then compared to astrophysically observed constraints and assessed regarding its quality and meaning.

2 Theoretical Description

2.1 Dark Matter

The first hints that our universe incorporates matter invisible to our eyes and other optical instruments occured nearly a century ago, when Swiss astronomer Fritz Zwicky observed the Coma cluster. Using the virial theorem, he estimated the mass of the galaxy cluster to be much higher than traditional methods based on luminosity would have suggested, essentially implying that most of the mass in the cluster stems from "invisible matter" [1].

When in the 1970s Vera Rubin and others conducted a study on the rotation curves of 60 galaxies, they found more evidence backing up the notion of invisible matter governing the motion of celestial objects. Assuming that the stars within a galaxy mimic the rotational behaviour of the planets in our solar system, their rotational velocity $v(r)$ would only be defined by Newtonian gravity, giving

$$v(r) = \sqrt{\frac{Gm(r)}{r}} \tag{1}$$

with G being the gravitational constant, r the distance from the center and $m(r)$ the total mass within r. This implies that $v(r)$ should decrease proportionally to $1/\sqrt{r}$ with increasing distance from the galactic center. However, the rotational curves that have been observed showed not the imagined form but turned out to be "flat", meaning that they would increase until a maximum was reached where $v(r) \sim const.$ [2]. Thus, Rubin concluded that "mass, unlike luminosity, is not concentrated near the center of spiral galaxies" [3].

Since then, a lot more astronomical and cosmological evidence was presented in favor of the general concept of dark matter, bringing us to the point where we can now assume ordinary, baryonic matter to only account for about 5% of the overall energy density of the universe, whereas the contribution of dark matter seems to be about five times higher. This paves the way for the search for suitable candidates that constitute dark matter. Research in this area was, for many decades, mainly governed by a focus on possibly detecting *WIMPs*, assuming *Weakly Interacting Massive Particles*, which are theoretically appealing because of numerous properties that are in concordance with the observations [1].

However, as the search for them did not yet show the desired results, a recent approach consists of studying a possible *SIMP* scenario, in which *Strongly Interacting Massive Particles*, as the name implies, interact with each other via a force similar to the strong nuclear force but not with the electromagnetic field [4]. There are numerous theories regarding the detailed structure of *SIMP* dark matter, many of whom can be shown to agree with the current observational indications just as well as a *WIMP* theory. This field is where this work is situated, with the underlying theory being further explained in the following subsections.

2.2 Underlying Lattice Gauge Theory

The *SIMP* theory explored in this work assumes a hidden sector described by a QCD-like gauge theory. A gauge theory in physics generally describes any theory where the Lagrangian is invariant under certain gauge transformations [5]. In this case, the transformations are elements of the gauge group $Sp(4)$. The technical details of this theory are provided in [6].

The field theory is formulated on a lattice, which allows for the use of non-perturbative techniques and simulations. This approach consists of defining a space-time lattice with discretized coordinates, giving for example

$$x = an, \quad n \in \mathbb{N} \tag{2}$$

for the spatial coordinate x with a being the lattice spacing (or lattice constant). This implies that physical quantities on the lattice (like scalar fields) are only defined on lattice points. Furthermore, a popular choice followed in this work is to consider only a lattice of finite volume with periodic boundary conditions, described for a scalar field $\phi(x)$ and $n = 0, 1, 2 \dots L-1$ by:

$$\phi(x) = \phi(x + aL) \tag{3}$$

The physical case of a continuous and infinite space-time would then arise in the limit of an infinite volume with $a \to 0$ [5].

In this work, a lattice with three spatial and one temporal dimension was simulated, having the following size:

$$L_i = 12, \quad i \in [1, 2, 3] \tag{4}$$

$$T = 24 \tag{5}$$

$$a = 1 \tag{6}$$

Here, L and T are the spatial and temporal lattice extents and a is the lattice constant.

A final note on the nomenclature used in this work: Since the investigated theory has strong similarities to QCD, the studied mesonic particles are named analogously. Hence, when π, ρ or a_0 particles are discussed, not their respective counterparts in QCD are meant (e.g. *the* pion), but their manifestations in the framework of this theory.

2.3 Correlation Functions and Obtainable Parameters

The primary observable that has been investigated in this work is the so-called correlation function or correlator of the simulated states. This quantity is built on the concept of the propagator in quantum mechanics.

Looking at its integral representation in quantum mechanics, the wave function for a particle at a certain position $\mathbf{x}''$ and time t can be expressed as

$$\psi(\mathbf{x}'', t) = \int K(\mathbf{x}'', t; \mathbf{x}', t_0)\psi(\mathbf{x}', t_0)d^3x' \tag{7}$$

where $\psi(\mathbf{x}', t_0)$ describes the wave function at an earlier time t_0 and another position $\mathbf{x}'$. Here, K is an integral kernel called the *propagator*, which is given by

$$K(\mathbf{x}'', t; \mathbf{x}', t_0) = \sum_{a'} \langle \mathbf{x}'' | a' \rangle \langle a' | \mathbf{x}' \rangle \exp\left\{ -\frac{iE_{a'}(t - t_0)}{\hbar} \right\} \tag{8}$$

with $E_{a'}$ and $|a'\rangle$ being the eigenenergies and eigenkets of the Hamiltonian operator. This can also be expressed as

$$K(\mathbf{x}'', t; \mathbf{x}', t_0) = \langle \mathbf{x}'', t | \mathbf{x}', t_0 \rangle \tag{9}$$

with $\langle \mathbf{x}'', t|$ and $|\mathbf{x}', t_0\rangle$ being eigenbras and eigenkets of the position operator. This in turn leads to the interpretation of the propagator as "transition amplitude": All the propagator (and hence our correlation function) does is give the amplitude for a particle to go from a space-time point $(\mathbf{x}', t_0)$ to the point $(\mathbf{x}'', t)$ [7].

In the following, the correlator will be denoted by $C(t)$. On a lattice, the correlation function takes only descrete values, as was mentioned earlier. In our case, being a sum of two exponential functions with different signs in the exponent, it takes on the form of a cosh function. The function that the correlators were fitted against reads

$$C(t) = \frac{f^2 m}{2L^3}(e^{-mt} + e^{-m(T-t)}) \tag{10}$$

with m, f being the mass and the decay constant of the described particle and T, L the total temporal and spatial lattice extents [8].

Since we have measured these correlators for a single π-meson ($C_\pi(t)$) as well as a state consisting of two π-mesons ($C_{\pi\pi}(t)$), we can define a ratio R as

$$R(t + a/2) = \frac{C_{\pi\pi}(t) - C_{\pi\pi}(t + a)}{C_\pi(t)^2 - C_\pi^2(t + a)} \tag{11}$$

where a is the lattice constant and in our case $a = 1$. This quantity shows the following behaviour for large times

$$R(t + a/2) = A_R[\cosh(\delta E_{\pi\pi} t') + \sinh(\delta E_{\pi\pi} t') \coth(2 \cdot m_{\pi\pi} t')] \tag{12}$$

with a factor A_R, the energy shift $\delta E_{\pi\pi}$ and $t' = t + a/2 - T/2$ [9].

From this, the scattering length a_0 of the $\pi\pi$-state can be determined by solving the equation [9]

$$\delta E_{\pi\pi} = \frac{4\pi a_0}{mL^3}\left(1 + c_1\frac{a_0}{L} + c_2\frac{a_0^2}{L^2}\right) \tag{13}$$

with the constants c_1 and c_2 having the known values [10]:

$$c_1 = -2.837297 \tag{14}$$

$$c_2 = 6.375183 \tag{15}$$

This finally leads us to the geometric cross section, which can be calculated using [7]:

$$\sigma = \pi a_0^2 \tag{16}$$

3 Aim and Methodology

The aim of this work is twofold, the primary question being whether or not the studied correlation functions are of reasonable quality and thus usable for further investigations. If this is the case, the follow-up question consists of probing whether the investigated particles then represent suitable candidates for dark matter. In order to answer these questions, the following methods were used:

First, the dark quark fields, constructing the studied meson states, were simulated on a lattice, incorporating the theoretical assumptions made earlier. The complete description of how the data were generated can be found in [6]. Here, the dark quark masses were non-degenerate in the case of the first simulations in section 4, whereas the second part, describing the scattering state of two dark pions in section 5, was simulated using mass-degenerate fields.[1]

In each case, a series of measurements was conducted where at each step the correlation function for every point along the time dimension was measured. From this data, the final correlators were extracted by taking the mean over all measurements $\overline{C(t)}$. The associated errors were calculated as the standard errors of the means according to [2]

$$\Delta\overline{C(t)} = \frac{\sigma}{\tau\sqrt{N}} \tag{17}$$

where σ is the standard deviation, N the number of measurements and τ a factor to account for autocorrelation, which was estimated to be $\tau = 2$ in the non-degenerate case and $\tau = 3$ for the mass-degenerate data set.

To obtain a first guess for the mass, the so-called effective mass

$$m_{eff}(t) = \log\left|\frac{C(t)}{C(t+1)}\right| \tag{18}$$

was computed and fitted to a constant in the region where its curve showed a plateau. To get an estimation of the fit error, the error bars of the data points were fitted as well and the resulting difference was taken to be the confidence interval for the fit.

Subsequently, the correlation functions themselves were fitted to Equation 10 using a non-linear least squares fit strategy, with free parameters being f and m. The confidence intervals were computed the same way as previously explained. The errors of the fit parameters were obtained by analysing the respective covariance matrices, while taking the statistical errors of the correlators into account. Thereby, the masses of the mesons (and in the case of the non-degenerate π particles, their decay constants as well) could be extracted.

[1] Mass degeneracy refers to the concept of constituting quark masses being either equal (*degenerate*) or not.

[2] The mean of the correlator $\overline{C(t)}$ from now on will just be referred to as $C(t)$, for the sake of clarity.

In the case of the mass-degenerate scattering state, further analysis was conducted, whereof the theoretical background has already been mentioned in subsection 2.3 and which will be described further in the following sections.

All analyses were carried out in Python using the libraries *numpy, scipy, pandas, matplotlib* and *seaborn*. All error estimations, if not stated otherwise, made use of error propagation theory, which was incorporated by using Python's *uncertainties* package.

4 Testing of Fit Strategy With Non-Degenerate Flavors

In order to test the fit strategy that has been implemented, the first step of the practical work consisted of fitting a dataset that has already been evaluated in [8]. All necessary data files were provided by Fabian Zierler [11]. While fitting the correlation functions, the fit strategy and intervals have been gradually modified in order to lead to the previously obtained results.

The particles that have been investigated correspond to a π-meson, a ρ-meson and an a_0-meson, in charged ($^{\pm}$) and uncharged ($_0$) form respectively.

For each individual particle, the correlation function was plotted alongside its implied effective mass. For the latter quantity, a constant fit was done to acquire a first guess regarding the mass of the particle. Subsequently, the correlation functions were fitted. The fit intervals for all of the correlators were oriented around the start of those that were chosen to fit the effective masses, but expanded towards the center of the time vector (i.e. $t = 12$), in order to capture the behaviour for high values of t.

4.1 π-Meson

The fitted correlation functions of the charged and uncharged π-correlator as well as their effective masses are shown in Figure 1 and Figure 2. The resulting graphs show very small error bands and a good correspondence to their respective fits. For this type of meson, a renormalization factor Z_A has been estimated in order to calculate the decay constants as well as the masses [12]. It reads

$$Z_A(p, \beta) = 1 + \frac{(5/4) \cdot (-12.82 - 3) \cdot 8}{16 \cdot \pi^2} \cdot \frac{1}{\beta \cdot p} \tag{19}$$

with β the inverse coupling and p the expectation value of the plaquette.[3] In this case, $\beta = 6.9$ and p was computed from the data to be $p = 0.538 \pm 0.004$. In order to account for the prefactor in Equation 10, the raw data were additionally multiplied by a factor of L^3, specifically for this evaluation. The obtained values are shown in the plots and agree with the results of previous analyses.

4.2 ρ-Meson

The evaluation for the ρ-meson was carried out just as the one of the former π-meson, with the caveat that for the lack of a suitable renormalization factor, only the mass has been extracted from the correlators. The obtained plots are shown in Figure 3 and Figure 4.

[3] Here, β describes the coupling to the lattice and p is a gauge invariant expression. These quantities are used heavily in lattice gauge theories; [5] is recommended for further reading.

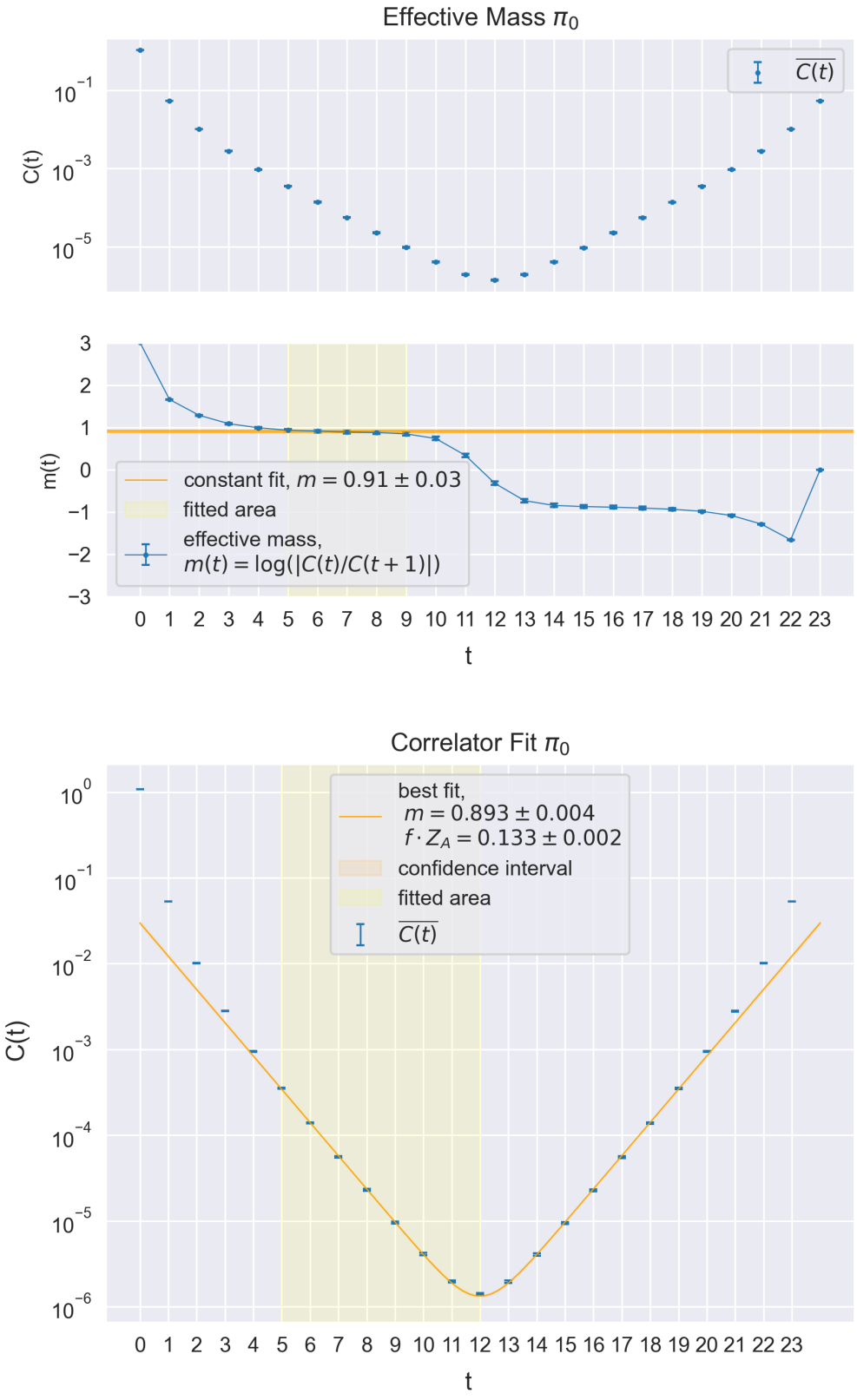

Figure 1: Effective mass and correlator fit for the π_0-correlator

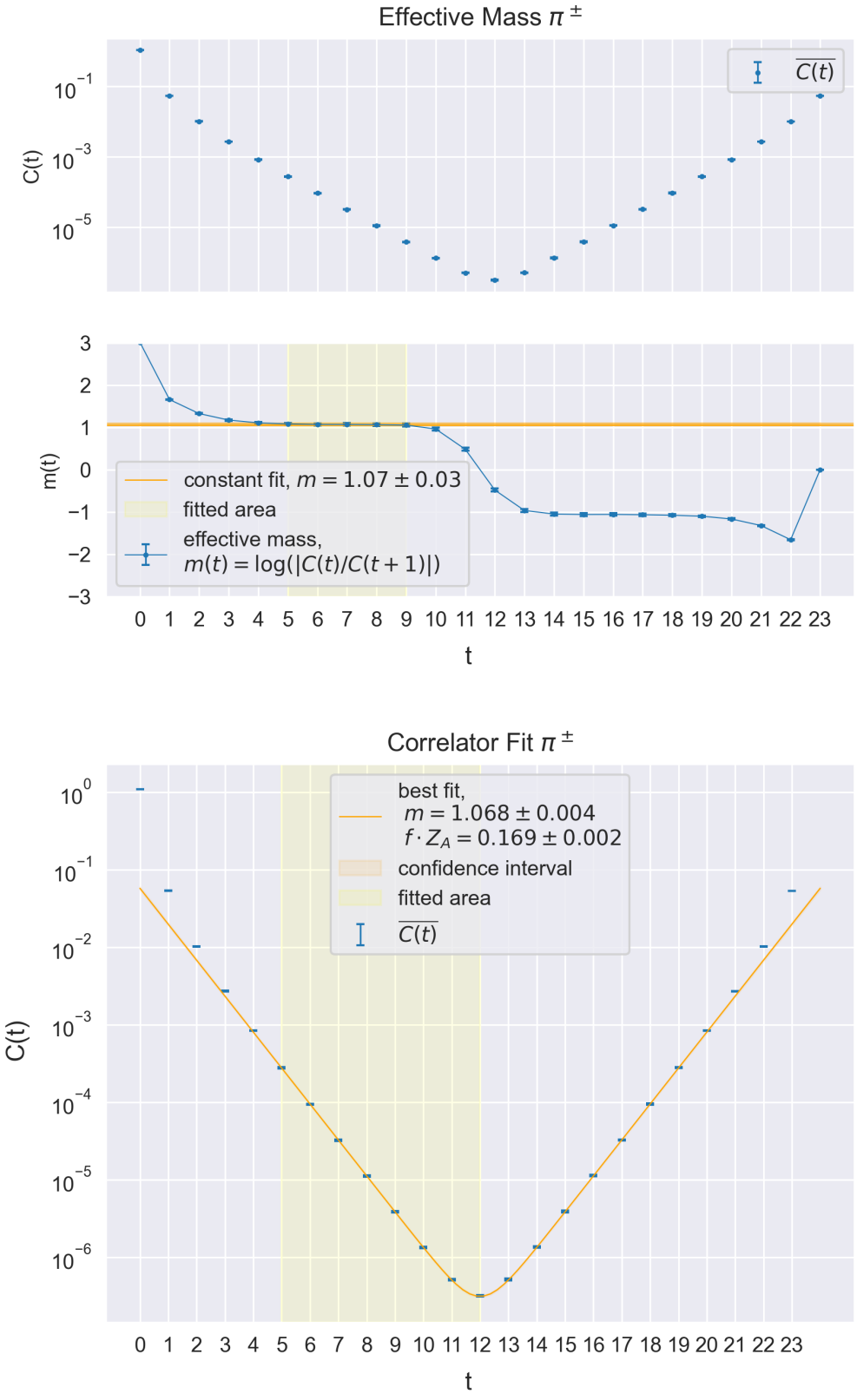

Figure 2: Effective mass and correlator fit for the $\pi^{\pm}$-correlator

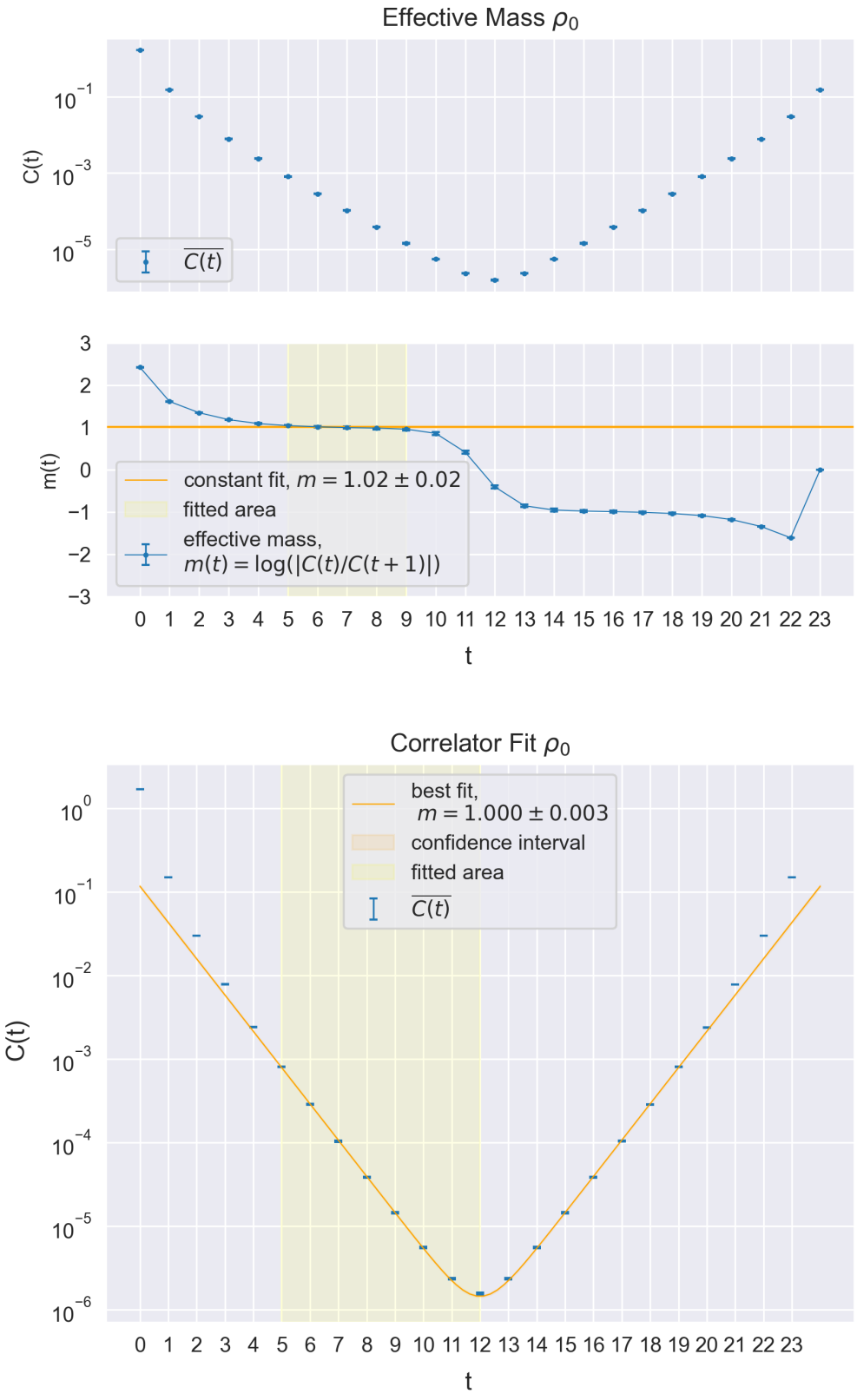

Figure 3: Effective mass and correlator fit for the ρ_0-correlator

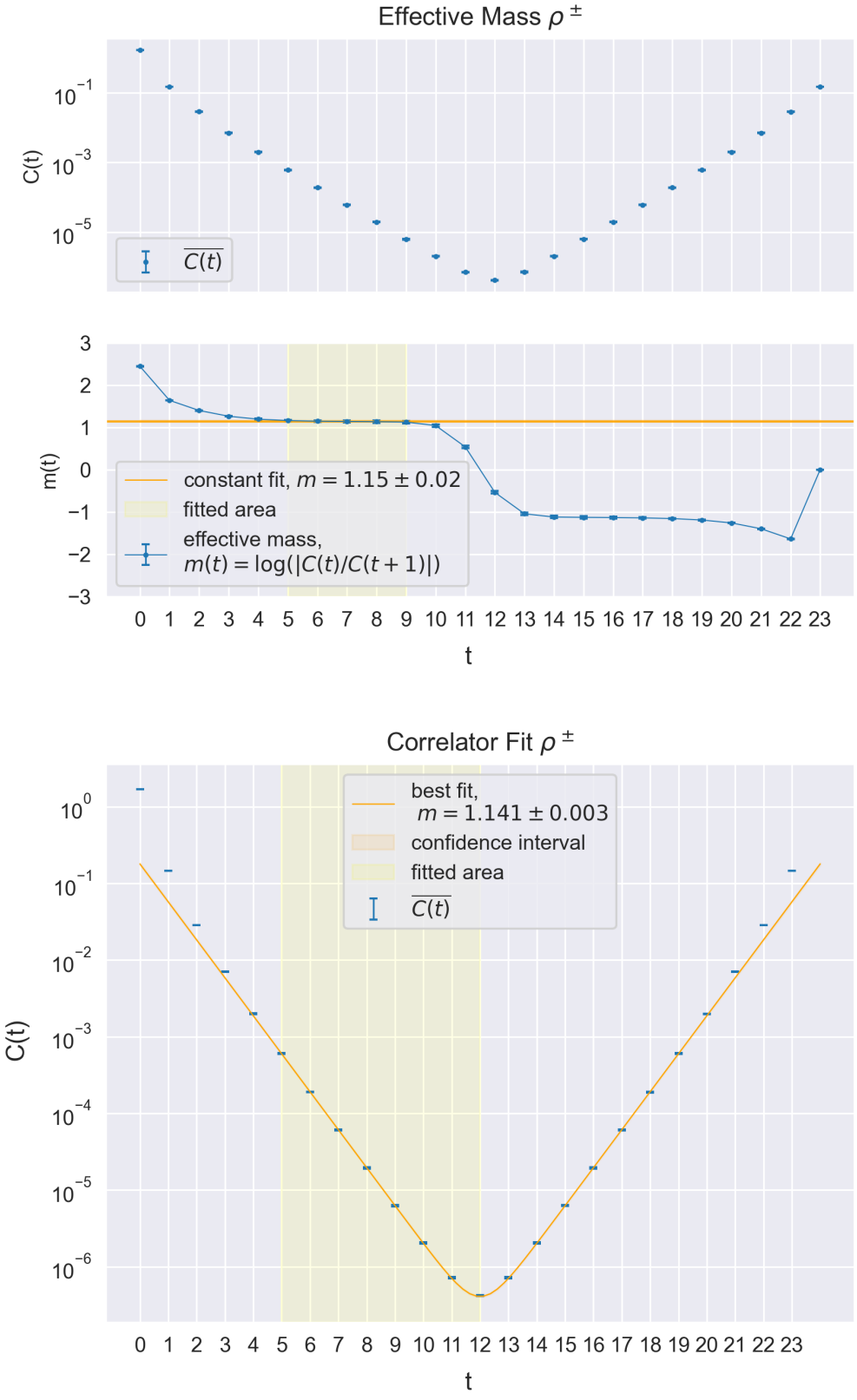

Figure 4: Effective mass and correlator fit for the $\rho^{\pm}$-correlator

4.3 a_0-Meson

The data of the a_0-meson has proven to be of a much poorer quality in terms of error margins, which is expected. Like with the ρ-meson, it was only possible to extract the mass of the particle from its correlation function. As can be seen, the errorbars are expanding rapidly towards large times, which is showcased in the following plots. However, the results have proven to align with those obtained earlier, and led to a conclusion in the testing of the fit strategy. The final plots are presented in Figure 5 and Figure 6.

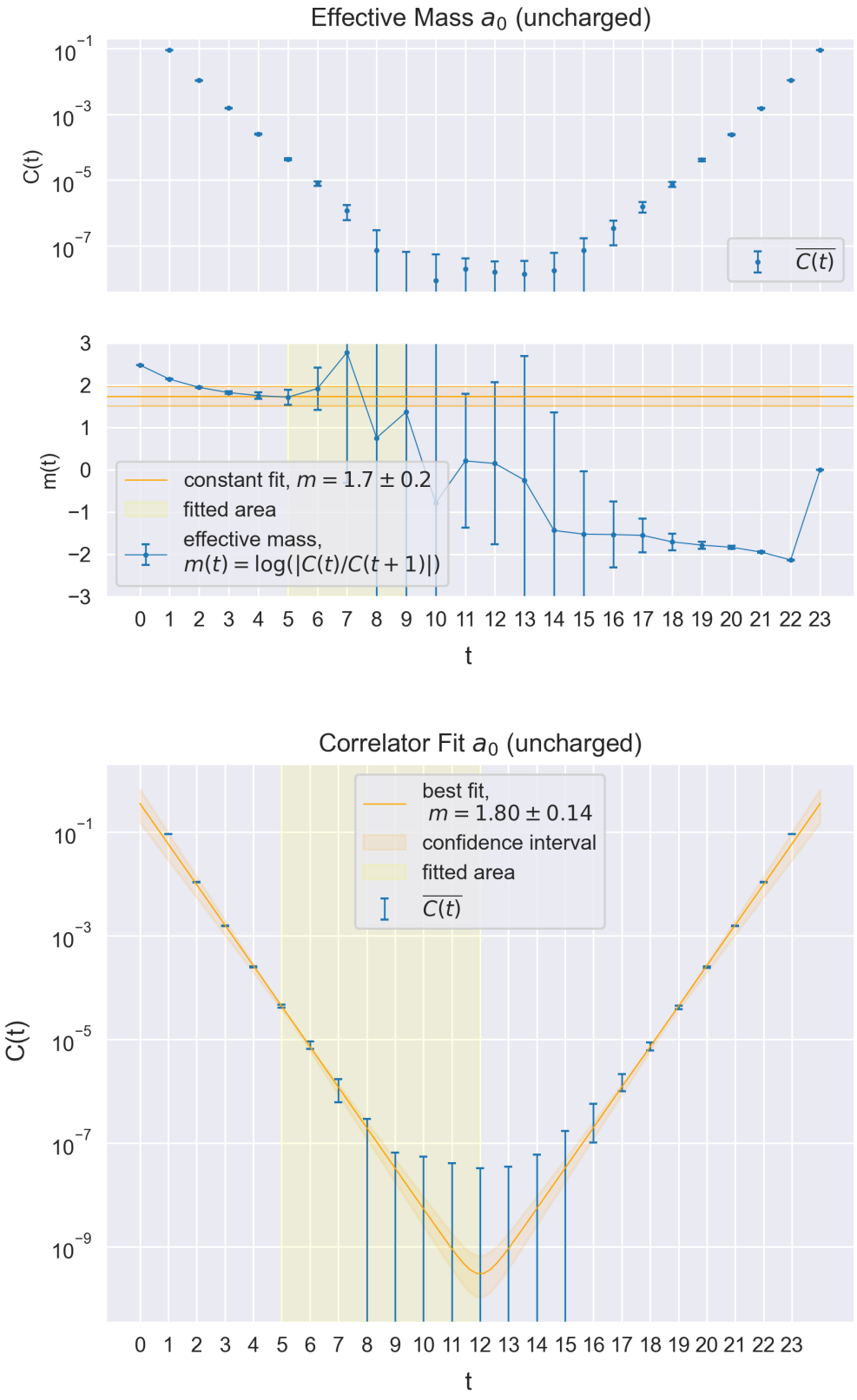

Figure 5: Effective mass and correlator fit for the uncharged a_0-correlator

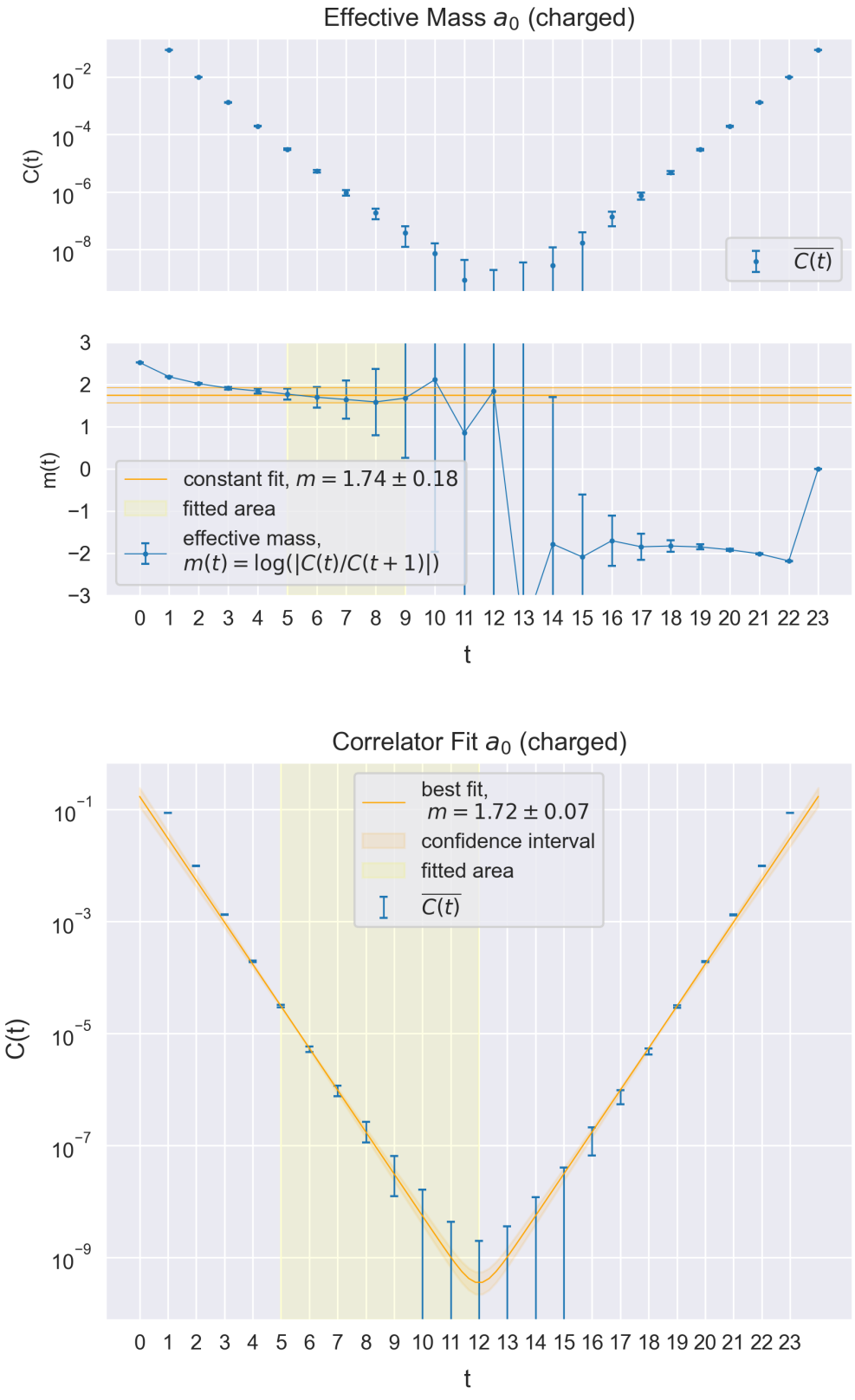

Figure 6: Effective mass and correlator fit for the charged a_0-correlator

5 Scattering State of Two Mass-Degenerate Flavors

After optimizing the fit strategy and testing with already analysed data, a new dataset has been generated, consisting of the correlation data for a single π-meson $C_\pi(t)$ as well as two particles with isospin 2 in an extreme low energy s-wave scattering state ($C_{\pi\pi}(t)$). These mesons have been simulated in a mass-degenerate case, implying that the differentiation between a charged and uncharged particle can be omitted.

5.1 Masses of $C_\pi(t)$ and $C_{\pi\pi}(t)$

First, the masses of the two correlation functions have been determined. For this, the respective correlation function has been prepared according to section 3. Then, the corresponding effective mass was plotted to provide a first guess for the mass, which can be seen in Figure 7 and Figure 8.

The correlation function $C_{\pi\pi}(t)$ was given in four parts, which construct the whole correlator additively and appear in pairs of two, that have similar magnitudes. In this context, it is interesting to note that not all of them contribute equally to the correlator, which is dominated by the first and last part.

The fit of the single correlator $C_\pi(t)$ is pictured in Figure 7. It shows a strong concordance with the raw data and a small error margin. The extracted mass in lattice units for one π-meson then equals:

$$m_\pi = 0.5741 \pm 0.0005 \tag{20}$$

The fit of the double correlator $C_{\pi\pi}(t)$ can be examined in Figure 8. This one also shows to agree with the correlation data while diverging from it a little more towards the center (i.e. towards higher times). Its mass – expressing its ground state energy – is calculated to be:

$$m_{\pi\pi} = 1.0151 \pm 0.0016 \tag{21}$$

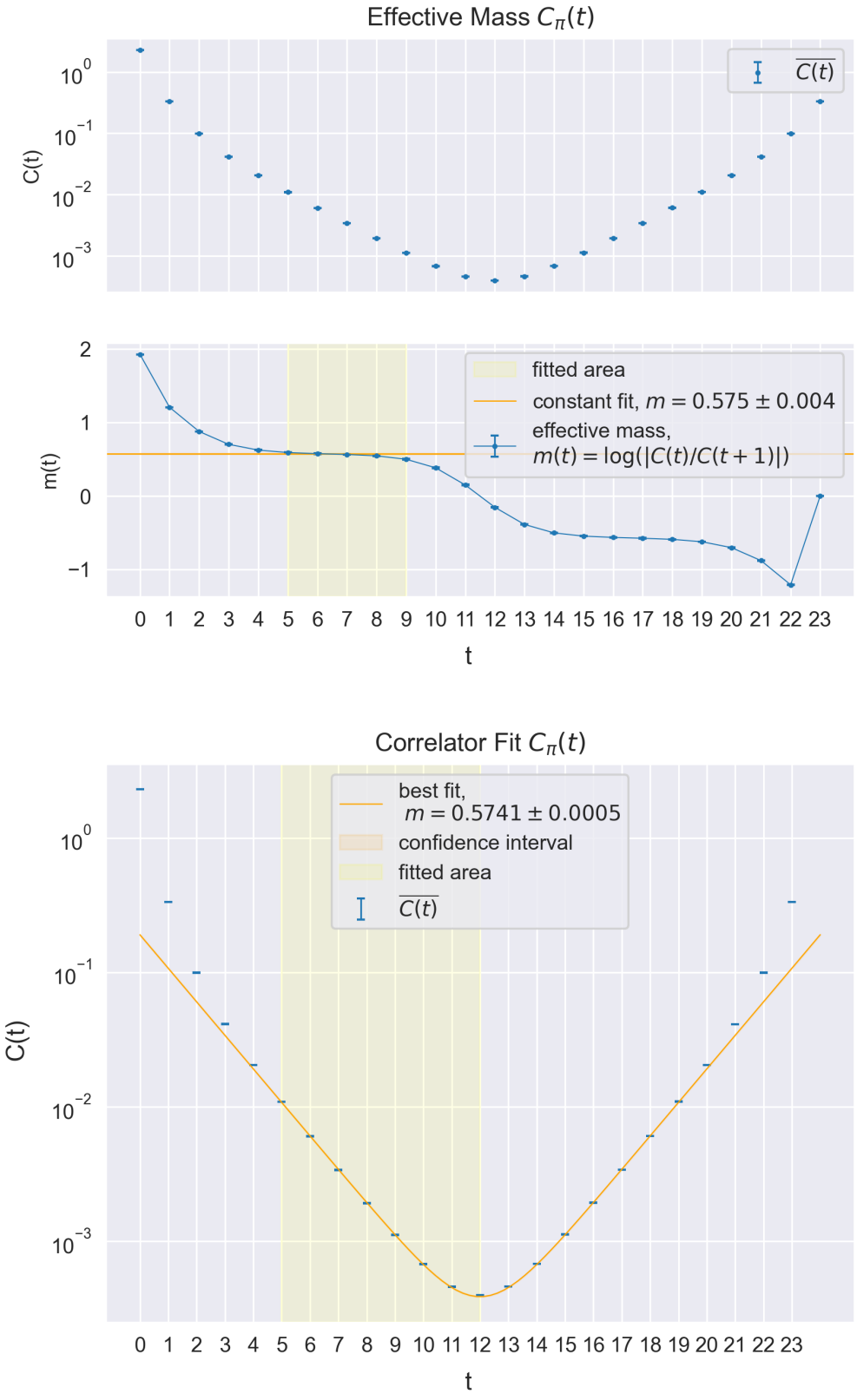

Figure 7: Effective mass and correlator fit for $C_\pi(t)$

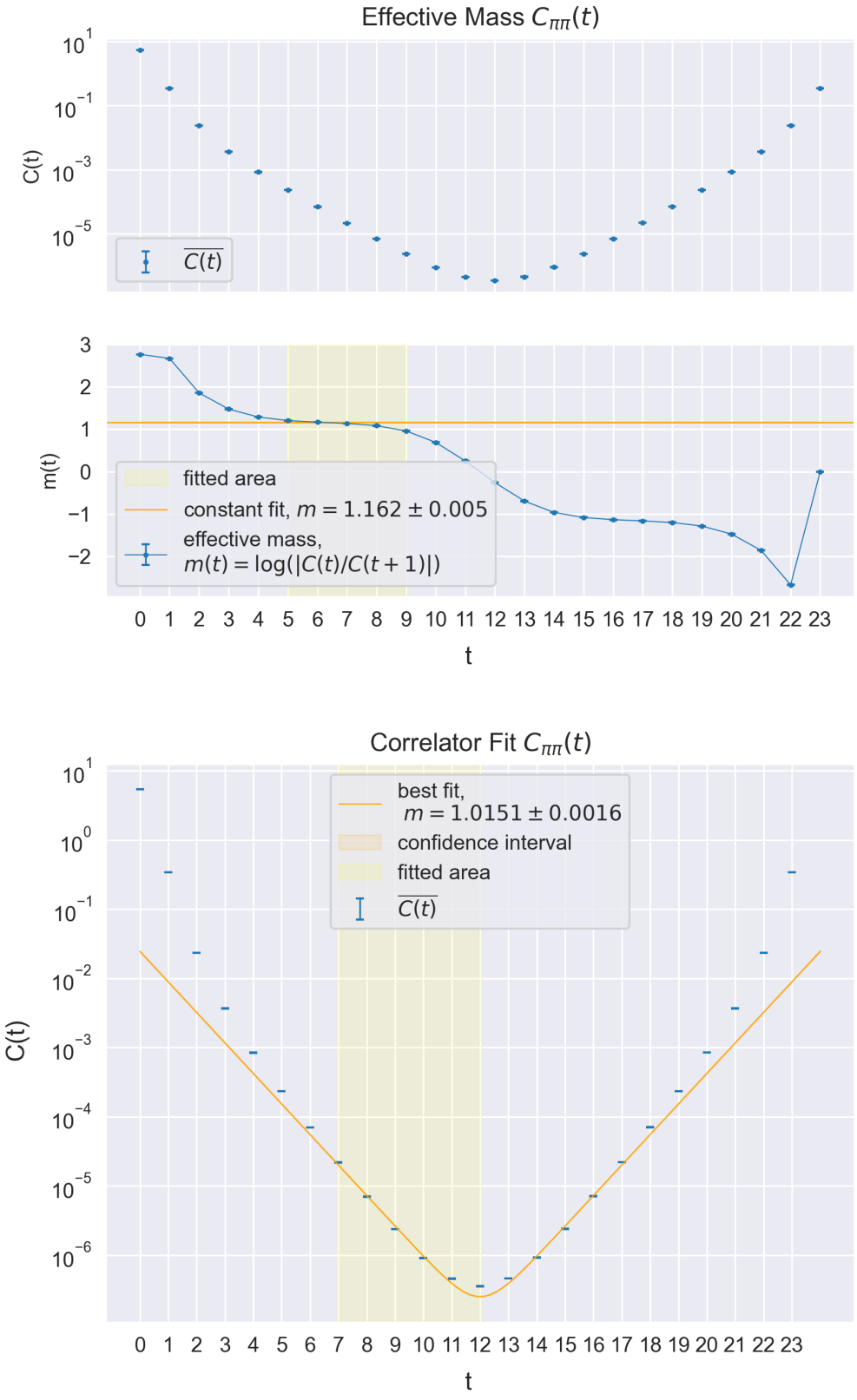

Figure 8: Effective mass and correlator fit for $C_{\pi\pi}(t)$

5.2 Extraction of Scattering Length and Cross Section

Lastly, the R ratio, that has been introduced earlier, was calculated using the provided correlators. A full plot of the resulting ratio is given in Figure 9.

In order to extract the scattering length of the assumed scattering state described by $C_{\pi\pi}(t)$, the R ratio was then fitted to Equation 12 according to the method that was introduced for the correlators in section 3, which is also shown in Figure 9. From this, the energy shift $\delta E_{\pi\pi}$ was found to be

$$\delta E_{\pi\pi} = 0.010 \pm 0.004 \tag{22}$$

and led – in combination with Equation 13 – to the scattering length in lattice units

$$a_0 = 1.0 \pm 0.5 \tag{23}$$

from which the cross section σ can be calculated using Equation 16. With an assumed mass for the single π-state, a scale can be introduced, and an equivalent of the scattering length in physical units can be found. This has been tried for $m_\pi = 100\,\mathrm{MeV}$ and $m_\pi = 1\,\mathrm{GeV}$, accompanied by a calculation of the respective cross sections. In accordance with their mathematical properties, the errors of the cross sections were computed as asymmetric intervals by variation of a_0 inside its error margins. The main results from this subsection in lattice units are listed in Table 1, their counterparts in physical units are shown in Table 2. The unit conversions were handled according to Appendix A of [13].

A frequently used measure to compare findings of this kind is the ratio of cross section to mass, which was also computed. Within the scale used, it is a dimensioned quantity, as can be seen by expanding the term, indicating a strong dependency on the pion mass:

$$\frac{\sigma}{m_\pi} = \frac{\pi a_{0,nat}^2}{m_{\pi,nat}} = \frac{\pi (a_{0,lat} \cdot a_{nat})^2}{m_{\pi,nat}} = \frac{\pi a_{0,lat}^2 \cdot m_{\pi,lat}^2}{m_{\pi,nat} \cdot m_{\pi,nat}^2} \tag{24}$$

Here, the subscript *lat* refers to quantities given in lattice units and shown in Table 1, whereas *nat* describes assumed or converted values in natural units, that are listed in Table 2. The studied mass range therefore leads to a possible range for the ratio of cross section to mass of about:

$$\frac{\sigma}{m_\pi} = \left(2.3^{+2.8}_{-0.6}\right) \cdot 10^{-n}\,\mathrm{cm}^2\,\mathrm{g}^{-1}, \quad n \in [1 \ldots 4] \tag{25}$$

Table 1: Main results given in lattice units
m_π ... mass of the single π-state
$m_{\pi\pi}$ ... mass of the $\pi\pi$-state
a ... lattice constant
a_0 ... scattering length
σ ... cross section

m_π	$m_{\pi\pi}$	a	a_0	σ
0.5741(5)	1.0151(16)	1	1.0(5)	$3.1^{+3.9}_{-0.8}$

Table 2: Scaled results for the $\pi\pi$-state given in natural units
m_π ... assumed mass for single π
a ... lattice constant
a_0 ... scattering length
σ ... cross section

m_π / GeV	a / GeV^{-1}	a_0 / GeV^{-1}	σ / GeV^{-2}	σ / mb
0.1	5.741(5)	6(3)	100^{+130}_{-30}	40^{+50}_{-10}
1	0.5741(5)	0.6(3)	$1.0^{+1.3}_{-0.3}$	$0.4^{+0.5}_{-0.1}$

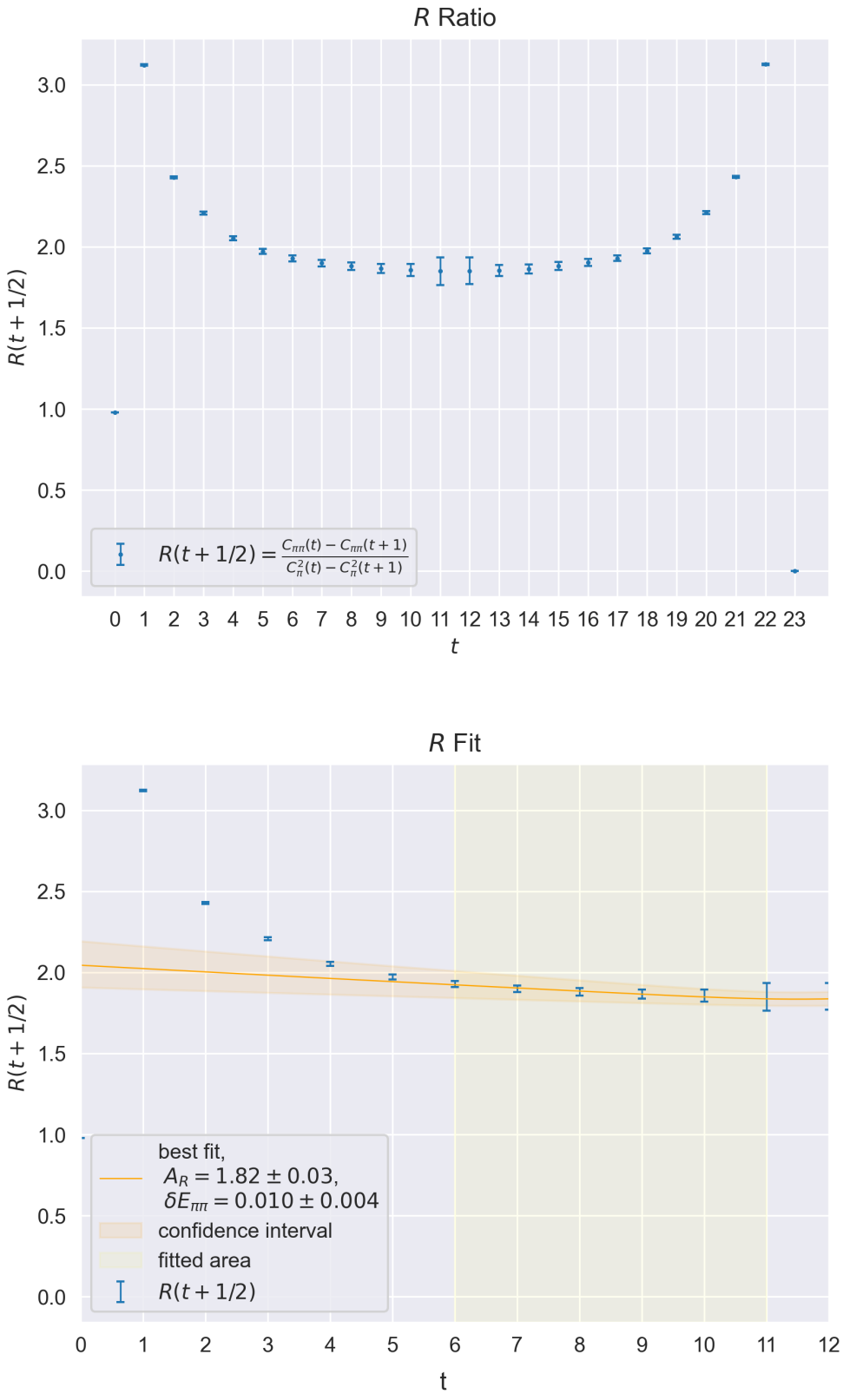

Figure 9: R ratio and fit in close-up view

6 Discussion of Results

The first step, consisting of developing a fit strategy suitable for analysing the relevant datasets, can be considered a success, since the already obtained results of [8] could be reproduced. The plots for the π- and ρ-mesons showed very small error bars and a very good correspondence to the fit. Providing a stark contrast, the data regarding the a_0 mesons had significantly higher error margins. However, since the obtained results for the masses were shown to have reasonable errors and still matched the expected ones, it can be assumed that the fit strategy was good enough to deal with the studied data and could be maintained for further analyses.

The correlators for the pions in the mass-degenerate case both again showed very good statistics, small error margins and were in good accordance with the fits. As can be seen, the extracted mass of $C_{\pi\pi}(t)$ is about 10% lower than the doubled $C_\pi(t)$ mass would be. This indicates a "loss" of energy in the simulation, thus hinting at an interaction happening between the π-mesons, corresponding to a scattering state.

The fit of R, despite said ratio also showing larger errors, led to very precise parameters. Regarding the following calculation of the scattering length, it should be noted that the values used for the coefficients c_1 and c_2 generally depend on the studied theory and thus cannot be guaranteed to give the correct results for this work. They should, however, provide a first guess regarding the order of magnitude of the scattering length, which is also how these results should be treated.

For the final calculation of the cross section, commonly assumed values for the mass of the dark pion were used. They led to a cross section to mass ratio of:

$$\sigma/m = \left(2.3^{+2.8}_{-0.6}\right) \cdot 10^{-n}\,\mathrm{cm}^2\,\mathrm{g}^{-1}, \quad n \in [1 \dots 4]$$

This, for example, lies well below the upper limit for self-interacting dark matter found from investigating merging galaxy clusters described as $\sigma/m < 1\,\mathrm{cm}^2\,\mathrm{g}^{-1}$ in [14]. Other astrophysical analyses, with a focus on probing dwarf galaxies with regard to the core-cusp problem, have found even lower upper boundaries like $\sigma/m < 0.19\,\mathrm{cm}^2\,\mathrm{g}^{-1}$ [15] and $\sigma/m < 0.13\,\mathrm{cm}^2\,\mathrm{g}^{-1}$ [16]. This hints at a dark pion mass greater than 100 MeV, since the ratio found for this value already lies outside the mentioned upper boundaries. In conclusion, the findings generally support the idea that the investigated strongly interacting particles could be viable candidates for dark matter.

7 Conclusion

In this exploratory work, a recently proposed scenario of strongly interacting dark matter particles in a QCD-like gauge theory has been studied. This was done by analysing the correlation functions of dark quark fields and thereby produced mesons in a lattice simulation. By conducting a non-linear least squares fit of these correlators, the masses of the investigated particles could be obtained.

For the case of two interacting particles in a mass-degenerate low energy scattering scenario, further analysis was conducted by examining the ratio R as defined in Equation 11 between the single- and double-π-correlators. By fitting this ratio for high values of t, an expression for the energy shift has been obtained that could be used to estimate the scattering length in the $\pi\pi$-state. By fixing the mass of the dark pion to certain values, a scale could be introduced and a range for possible cross sections was determined. The main results regarding these analyses are shown in Table 1 in lattice units and Table 2 in natural units. The cross section to mass ratio of the dark pions for an assumed pion mass in the range of $m_\pi = 100$ MeV to $m_\pi = 1$ GeV was found to be:

$$\sigma/m = \left(2.3^{+2.8}_{-0.6}\right) \cdot 10^{-n}\,\mathrm{cm}^2\,\mathrm{g}^{-1}, \quad n \in [1 \dots 4]$$

By comparing these findings to the experimental constraints put on dark matter candidates, one can see that the studied particles lie well within the possible range, if the dark pion mass is set high enough. Thus, it is concluded that the studied theory constitutes an interesting and promising approach for the search for dark matter particles and should be investigated more thoroughly. Furthermore, the correlation functions that have been examined in the mass-degenerate case were well suited for statistical analysis, provided usable insights and can thereby be regarded as a useful tool for further studies.

References

[1] C. Bambi and A. D. Dolgov, *Introduction to Particle Cosmology*. Springer Berlin Heidelberg, 2016. DOI: 10.1007/978-3-662-48078-6.

[2] K. Garrett and G. Duda, "Dark matter: A primer," *Adv.Astron.2011:968283,2011*, Jun. 2010. DOI: 10.1155/2011/968283. arXiv: 1006.2483 [hep-ph].

[3] V. C. Rubin, "Dark matter in spiral galaxies," *Scientific American*, vol. 248, no. 6, pp. 96–108, Jun. 1983. DOI: 10.1038/scientificamerican0683-96.

[4] Y. Hochberg, E. Kuflik, H. Murayama, T. Volansky, and J. G. Wacker, "The SIMPlest Miracle," *Phys. Rev. Lett. 115, 021301 (2015)*, Nov. 2014. DOI: 10.1103/PhysRevLett.115.021301. arXiv: 1411.3727 [hep-ph].

[5] G. Münster and M. Walzl, "Lattice gauge theory - a short primer," Dec. 2000. arXiv: hep-lat/0012005 [hep-lat].

[6] S. Kulkarni, A. Maas, S. Mee, M. Nikolic, J. Pradler, and F. Zierler, "Low-energy effective description of dark Sp(4) theories," Feb. 2022. arXiv: 2202.05191 [hep-ph].

[7] J. J. Sakurai and J. Napolitano, *Modern Quantum Mechanics*. Cambridge University Press, Sep. 2017. DOI: 10.1017/9781108499996.

[8] A. Maas and F. Zierler, "Strong isospin breaking in Sp(4) gauge theory," *PoS(LATTICE2021)130*, Sep. 2021. arXiv: 2109.14377 [hep-lat].

[9] R. Arthur, V. Drach, M. Hansen, A. Hietanen, C. Pica, and F. Sannino, "Scattering lengths in SU(2) gauge theory with two fundamental fermions," Dec. 2014. arXiv: 1412.4771 [hep-lat].

[10] M. Lüscher, "Volume dependence of the energy spectrum in massive quantum field theories," *Communications in Mathematical Physics*, vol. 105, no. 2, pp. 153–188, Jun. 1986. DOI: 10.1007/bf01211097.

[11] F. Zierler, *Private communication*.

[12] E. Bennett, D. K. Hong, J.-W. Lee, *et al.*, "Sp(4) gauge theories on the lattice: $N_f = 2$ dynamical fundamental fermions," *JHEP*, vol. 12, p. 053, 2019. DOI: 10.1007/JHEP12(2019)053. arXiv: 1909.12662 [hep-lat].

[13] M. Guidry, *Gauge Field Theories*. Wiley, Oct. 1991. DOI: 10.1002/9783527617357.

[14] M. Markevitch, A. H. Gonzalez, D. Clowe, *et al.*, "Direct constraints on the dark matter self-interaction cross section from the merging galaxy cluster 1e 0657-56," *The Astrophysical Journal*, vol. 606, no. 2, pp. 819–824, May 2004. DOI: 10.1086/383178.

[15] D. Eckert, S. Ettori, A. Robertson, *et al.*, "Constraints on dark matter self-interaction from the internal density profiles of X-COP galaxy clusters," May 2022. arXiv: 2205.01123 [astro-ph.CO].

[16] K. E. Andrade, J. Fuson, S. Gad-Nasr, *et al.*, "A stringent upper limit on dark matter self-interaction cross-section from cluster strong lensing," *Mon. Not. Roy. Astron. Soc.*, vol. 510, no. 1, pp. 54–81, 2021. DOI: 10.1093/mnras/stab3241. arXiv: 2012.06611 [astro-ph.CO].

List of Figures

List of Tables